Understanding the charge pumping and relaxation of the chiral anomaly in a Dirac semimetal

April 29 2021, by Thamarasee Jeewandara

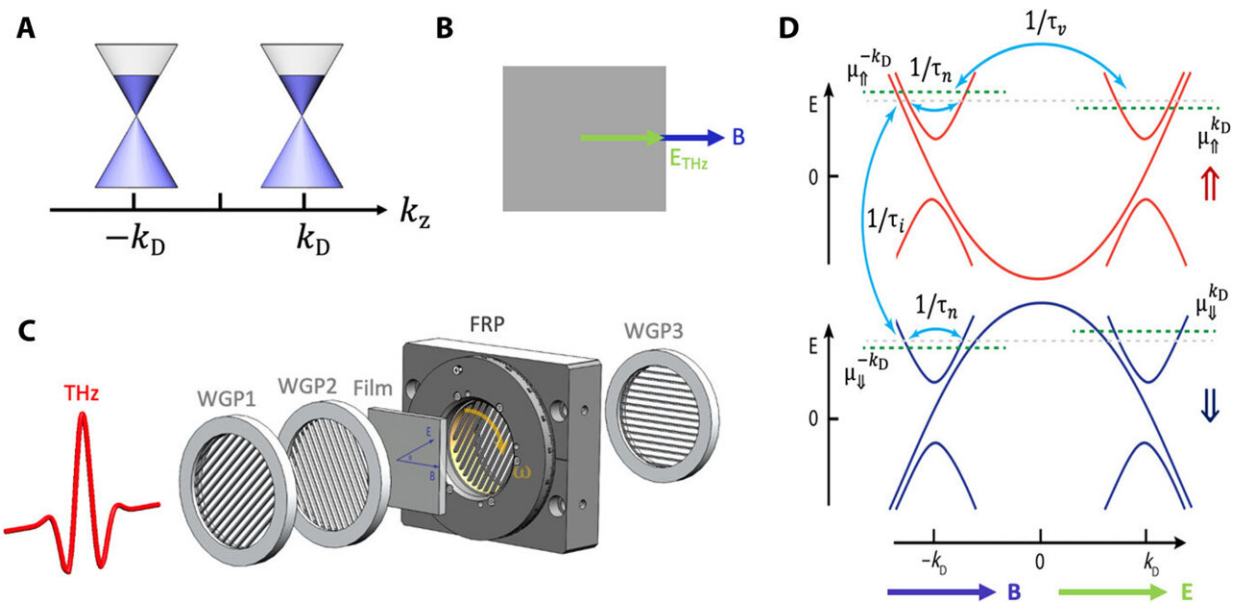

Charge dynamics of the chiral anomaly in a DSM and the experimental setup. (A) Schematic illustration of the low-energy electronic structure of the DSM Cd3As2. It hosts two 3D Dirac nodes located along the kz axis. (B) The chiral anomaly is expected when the dc magnetic field and the THz electric field are coaligned. (C) Schematic of the time domain magnetoterahertz spectrometer used to collect data. Wire grid polarizer 1 (WGP1) and WGP2 are used to produce linearly polarized terahertz pulse with ETHz ∥ B or ETHz ⊥ B. A fast rotation polarizer (FRP) is used to modulate terahertz electric field by a frequency near 47 Hz. With WGP3 and lock-in amplifier, the complex transmission matrix can be determined through a single measurement to high precision. (D) In a DSM with ETHz ∥ B, the 3D Dirac states will develop Landau

levels (LLs), which are dispersive along the direction of magnetic field. The zeroth LL gives the chiral current. A number of different relaxation rates control the charge dynamics. 1/τn is the intranode (normal) scattering rate, 1/τv is the intervalley scattering rate, and 1/τi is the internode scattering rate at the same momentum valley, but to the other isospin variety. Credit: Science Advances, doi:10.1126/sciadv.abg0914

The 3D Dirac and Weyl semimetals can be characterized by a charge chirality with the parallel or antiparallel locking of electron spin in its momentum. Such materials can exhibit a chiral magnetic effect associated with the near conservation of chiral charge. In this work, Bing Cheng and a research team in physics and astronomy at the Johns Hopkins University and materials science at the University of California, Santa Barbara, used magneto-terahertz spectroscopy to study epitaxial cadmium arsenide (Cd_3As_2) films—a widely explored material in solid-state physics to extract their conductivities as a function of chiral magnetic effect . When the team applied the field, they noted a markedly sharp Drude response – a highly acclaimed model of electronic transport suggested by physicist Paul Drude more than 100 years ago. The Drude response rose out of the broader background of this system as a definitive signature of a new transport channel consistent with the chiral response. The field independence of the chiral relaxation established that it was set by the approximate conservation of the isospin in the setup.

The chiral anomaly

Some of the most remarkable demonstrations of topological states of matter arise from their response to electromagnetic fields. For instance, topological insulators are characterized by a quantized magnetoelectric effect. Weyl semimetal and Dirac Semimetals (WSM and DSM) are

states of matter in which conduction and valence bands touch and disperse near-linearly around pairs of nodes in momentum space. Each node can be identified by its chirality relative to the spin of a massless (linearly dispersing) particle oriented parallel or antiparallel to its momentum. Dirac systems are therefore similar to two copies of the Weyl systems; at each node, there are two sets of the linearly dispensing bands with opposite chiral charge. Despite being metals, Weyl semimetals and Dirac semimetals showed distinct transport effects associated with the near conservation of chiral charge. The chiral anomaly therefore existed in the quantum and semiclassical transport limits. The chiral charge is not conserved in any real material due to violations of chiral symmetry via nonlinear band dispersions. As a result, the near conservation of chiral charge is relative to emergent low-energy chiral symmetry. While the effect existed in semiclassical and quantum transport regimes, the effect was most well understood in the quantum limit. The chiral charge is not precisely conserved and is pumped under the action of collinear electric and magnetic fields referred to as the chiral anomaly. Scientists have observed a negative longitudinal magnetoresistance (NLMR) in a number of Dirac semimetal and Weyl semimetal systems as a consequence of the chiral magnetic effect, although NLMR is not uniquely caused by this effect.

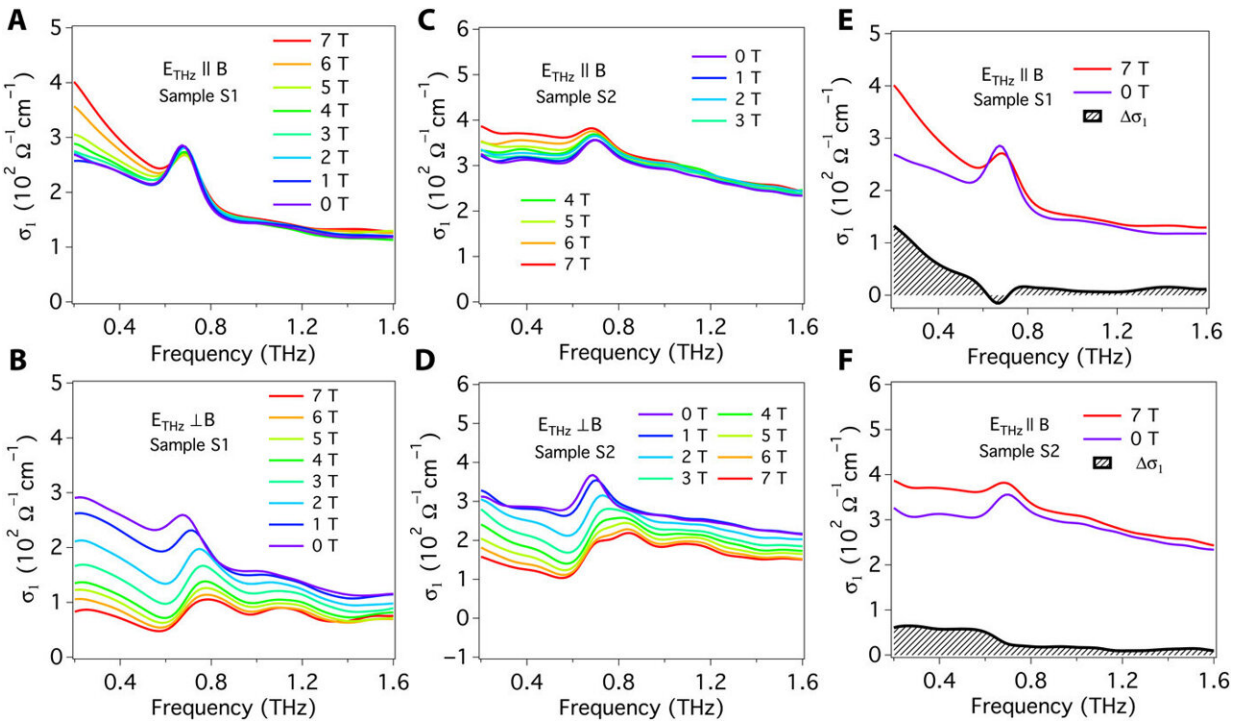

Terahertz conductivity at different magnetic fields. (A) ETHz ∥ B with B∥(1¯10) for sample S1. Chiral anomaly leads terahertz conductivity σ1 below 1 THz to be gradually enhanced by magnetic field. (B) ETHz ⊥ B with B∥(1¯10) for sample S1. The suppression of terahertz conductivity σ1 is the signature of positive magnetoresistivity, which is generally observed in perpendicular magnetic and electric fields. (C) ETHz ∥ B for B∥(11¯¯¯¯2) sample S2. (D) ETHz ⊥ B for B∥(11¯¯¯¯2) sample S2. (E and F) Comparisons of this 0- and 7-T data and their differences for samples S1 and S2. Δσ1 is the intrinsic chiral conductivity from chiral anomaly. The highlighted gray area represents the strength of charge pumping effect, and its width defines the chiral relaxation rate. Credit: Science Advances, doi:10.1126/sciadv.abg0914

The experiments

A key parameter governing the chiral anomaly is the chiral relaxation rate. The intrinsic properties of the chiral anomaly can be most

convincingly characterized by directly measuring the chiral relaxation rate and intravalley relaxation rates. King et al. used magneto-terahertz spectroscopy to study the high-quality epitaxial thin films of Dirac semimetals cadmium arsenide (Cd_3As_2). This is an ideal material for investigations due to its quadruple degenerate Dirac nodes that are protected by a C_4 symmetry. Typically, the high-quality oriented Cd_3As_2 films can be grown using molecular beam epitaxy. By performing frequency dependent conductivity experiments, the scientists extracted both the chiral relaxation rate and intravalley relaxation rates directly. They then measured two Cd_3As_2 films and extracted their field-dependent terahertz conductivity using two contactless measurements to avoid any artefacts associated with the inhomogeneous current paths that tend to plague direct current experiments.

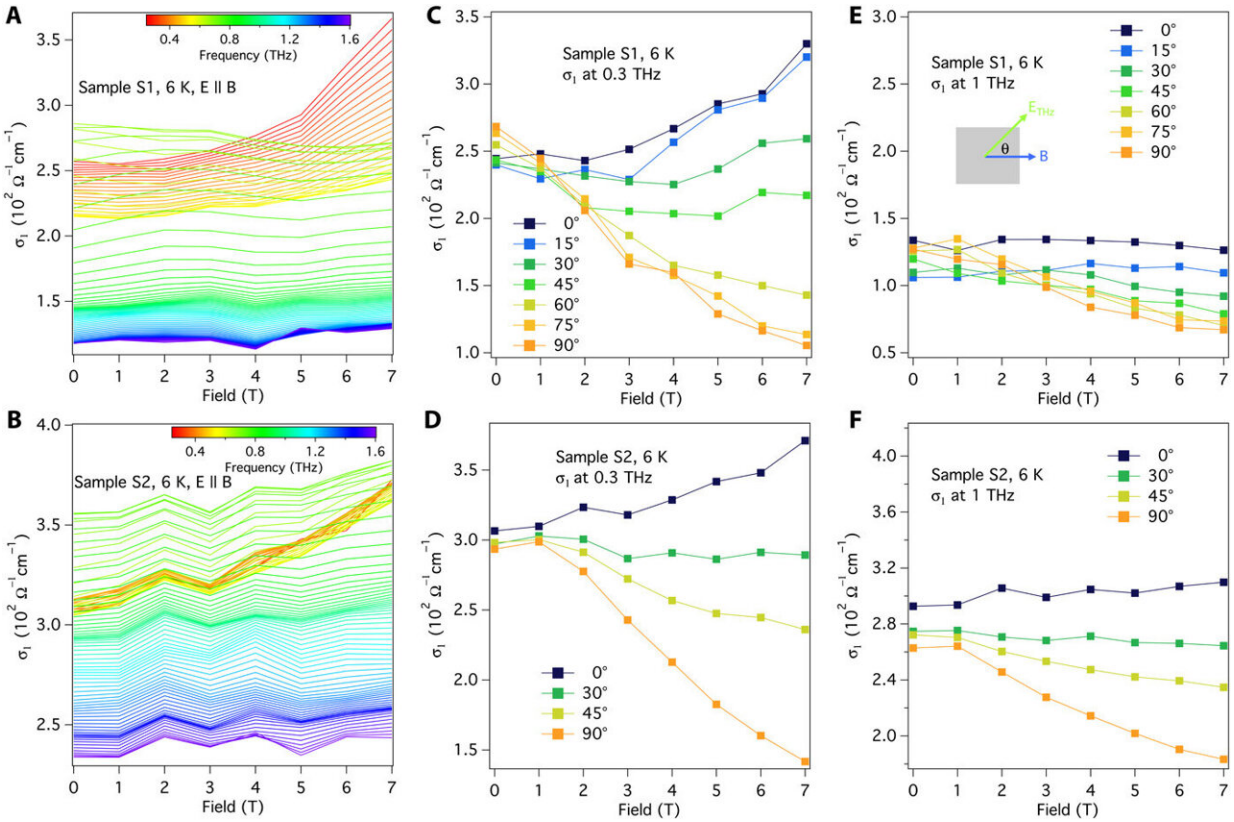

Terahertz conductivity at different magnetic fields. Terahertz conductivity σ1 at each frequency (see color bar scale) as a function of magnetic field of (A) sample S1 and (B) sample S2 with ETHz ∥ B. Terahertz conductivity (at 0.3 THz) as a function of magnetic field under different terahertz polarization angles of (C) sample S1 and (D) sample S2. The configuration of polarization angle θ between terahertz electric field and magnetic field is shown by the schematic in (E). Terahertz conductivity (at 1 THz) as a function of magnetic field under different terahertz polarization angles of (E) sample S1 and (F) sample S2. All data were taken at 6 K. Credit: Science Advances, doi:10.1126/sciadv.abg0914

Terahertz conductivity and chiral transport

The team next investigated terahertz conductivity at different magnetic fields and extracted the dynamic charge pumping and relaxation of the chiral anomaly using Drude-Lorentz fits. They noted a remarkable field-induced effect resulting in an enhancement of only the low-frequency conductivity. However, this did not result from a change in the normal scattering rate or change in carrier density of the material but relied on the appearance of a parallel transport channel with a new frequency scale. The effect was also not associated with spin-dependent scattering, which would usually manifest as an overall change in the scattering rate. The appearance of an additional transport channel and new timescale was precisely in agreement with the theoretical expectations for the chiral anomaly. Chiral transport occurred via a build-up of the effective electrochemical potential through the balance between chiral pumping and internode scattering. To distinguish a steady-state chiral current, the chiral scattering rate had to be smaller than the intravalley relaxation rate. In the experiments, Cheng et al. noted the chiral scattering rate to be approximately one-fourth of the intravalley relaxation rate in both samples. The scientists compared this relative size in light of prevailing theory and expect to conduct further studies in this area in the future. The team also interpreted the recent nonlinear terahertz experiments

relative to chiral relaxation that showed a slow rate due to larger separation of nodes in the Weyl semimetal crystalline tantalum arsenide (taAs) and/or the lack of isospin scattering.

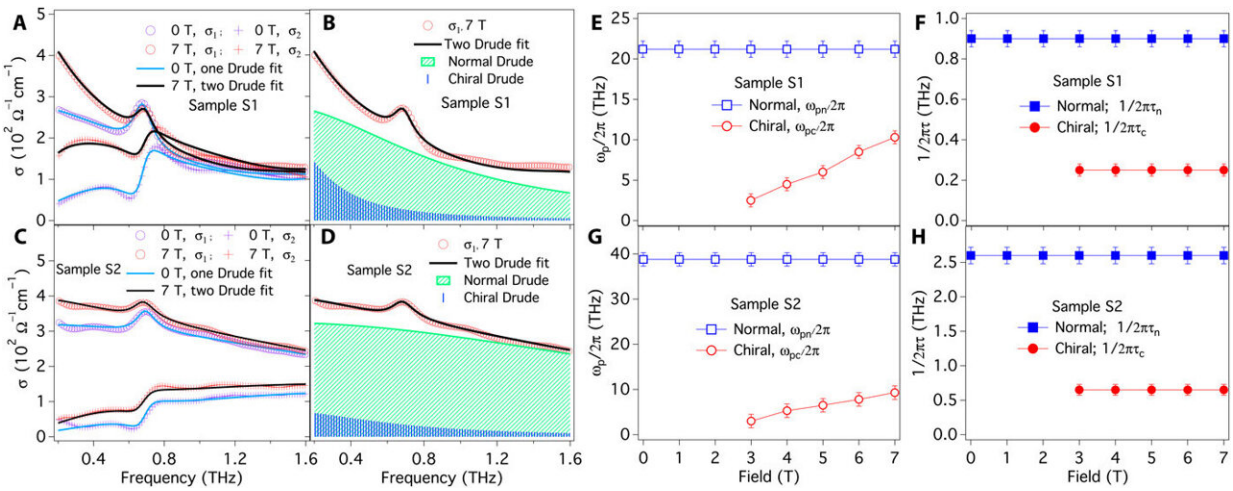

Dynamical charge pumping and relaxation of the chiral anomaly extracted by Drude-Lorentz fits. (A and B) Fits to terahertz conductivity of sample S1 with ETHz ∥ B. The sharper Drude oscillator (blue shadowed area) represents the new transport channel from chiral anomaly. (C and D) Fits to terahertz conductivity of sample S2 with ETHz ∥ B. Field-dependent Drude plasma frequency in sample S1 (E) and sample S2 (G). The plasma frequencies of chiral transport channel (ωpc/2π, red) directly correspond to chiral charge pumping and are linear functions of field. Scattering rates in sample S1 (F) and sample S2 (H). The chiral scattering rates (1/2πτc, red) control the dynamical process of chiral anomaly as shown in Fig. 1D, and in both samples, they are much smaller than normal bulk scattering rates (1/2πτn, blue). Credit: Science Advances, doi:10.1126/sciadv.abg0914

Outlook

In this way, Bing Cheng and colleagues observed an anomalous terahertz

magnetoconductivity effect in the Dirac semimetal cadmium arsenide. The effect depended on the chiral magnetic effect. The observed dependence and evolution of the functional form of conductivity was in precise agreement with the theory of chiral anomaly. However, the rates of chiral scattering and intranode scattering were not precisely in agreement with the prevailing theory since chiral scattering was much stronger than predicted. The researchers will therefore develop more revised models with more realistic rates of experimental impurity scattering in the future.

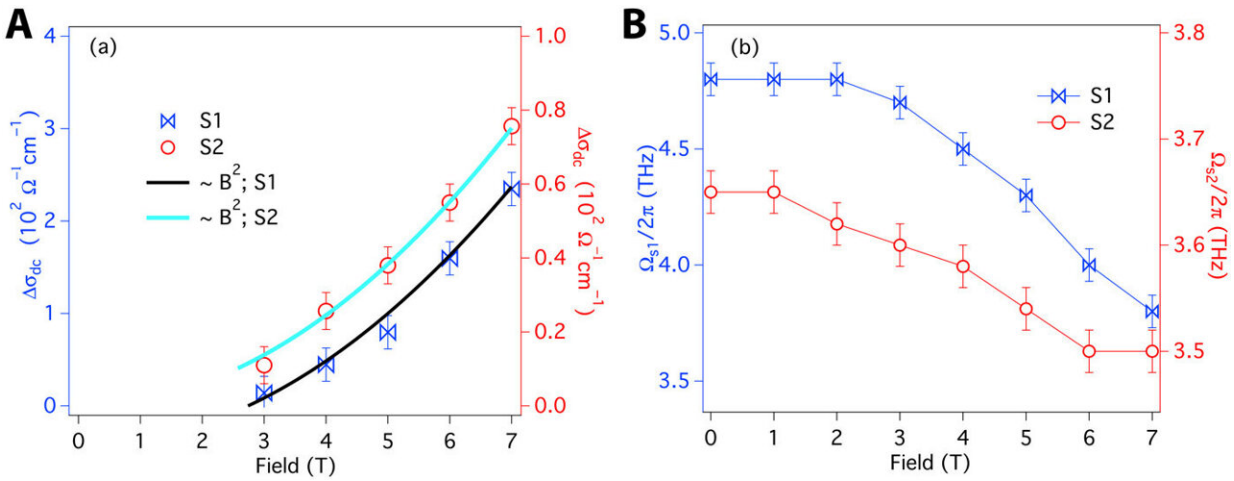

Intrinsic dc chiral conductivity extrapolated from terahertz conductivity. (A) Intrinsic dc magnetoconductivity from chiral anomaly in sample S1 (blue) and sample S2 (red). In both samples, Δσ follows B2, consistent with the prediction of field dependence of chiral current in semiclassical transport regime. (B) Phonon oscillator strength in sample S1 (blue) and sample S2 (red). The oscillator strengths in both samples decrease as the chiral conductivity is enhanced by magnetic field. Credit: Science Advances, doi:10.1126/sciadv.abg0914

More information: Cheng B. et al. Probing charge pumping and relaxation of the chiral anomaly in a Dirac semimetal, *Science Advances*, 10.1126/sciadv.abg0914

Wu L. et al. Quantized Faraday and Kerr rotation and axion electrodynamics of a 3D topological insulator, *Science*, 10.1126/science.aaf5541

Parameswaran S. A. et al. Probing the chiral anomaly with nonlocal transport in three-dimensional topological semimetals, *Physical Reviews X* doi.org/10.1103/PhysRevX.4.031035

© 2021 Science X Network

Citation: Understanding the charge pumping and relaxation of the chiral anomaly in a Dirac semimetal (2021, April 29) retrieved 25 April 2024 from https://phys.org/news/2021-04-chiral-anomaly-dirac-semimetal.html

This document is subject to copyright. Apart from any fair dealing for the purpose of private study or research, no part may be reproduced without the written permission. The content is provided for information purposes only.